Journal of Antimicrobial Chemotherapy (2008) **61**, 323–331
doi:10.1093/jac/dkm485
Advance Access publication 21 December 2007

JAC

Altered expression of isoniazid-regulated genes in drug-treated dormant *Mycobacterium tuberculosis*

Petros C. Karakousis[1,2]*, Ernest P. Williams[1] and William R. Bishai[1,2]

[1]*Center for Tuberculosis Research, Division of Infectious Diseases, Johns Hopkins University School of Medicine, Baltimore, MD, USA;* [2]*Department of International Health, Johns Hopkins Bloomberg School of Public Health, Baltimore, MD, USA*

Received 28 August 2007; returned 12 October 2007; revised 25 October 2007; accepted 14 November 2007

***Objectives*: Despite having potent activity against actively replicating *Mycobacterium tuberculosis*, isoniazid has very limited activity against dormant bacilli. In order to investigate the lack of bactericidal activity of this drug under conditions leading to mycobacterial dormancy, we studied the transcriptional pattern of *M. tuberculosis* in different physiological states following exposure to isoniazid.**

***Methods*: Global gene expression analysis was used to study *M. tuberculosis* treated with isoniazid in dormancy models of nutrient depletion and progressive hypoxia *in vitro*, as well as in an *in vivo* hollow fibre model of dormancy. Mycobacterial expression of the drug's putative transcriptional signature was investigated by RT–PCR in each dormancy model, and during the early and chronic phases of infection in the mouse aerosol model. Transcriptional responses were correlated with the bactericidal activity of isoniazid in the respective models.**

***Results*: A small group of genes directly relevant to the mechanism of action of isoniazid was confirmed to constitute a transcriptional signature of the drug, as differential regulation of these genes was abrogated in an isoniazid-resistant, *katG*-deficient *M. tuberculosis* strain following isoniazid exposure. Isoniazid-induced expression of this transcriptional signature was abolished in dormant bacilli which had acquired phenotypic tolerance to isoniazid, regardless of the specific conditions responsible for the induction of the dormancy phenotype. Quantitative RT–PCR revealed that expression of isoniazid-regulated genes (IRGs) is dramatically altered under conditions of nutrient depletion and progressive hypoxia *in vitro*. Although these IRGs are highly induced following drug exposure early in infection in the mouse hollow fibre and aerosol models, correlating with potent bactericidal activity of the drug, their expression levels are markedly diminished during late-stage infection in these two models, coinciding with the greatly reduced bactericidal activity of isoniazid against these organisms.**

***Conclusions*: The reduced susceptibility of bacilli to the bactericidal drug isoniazid, as well as lack of expression of IRGs upon exposure to the drug, may be defining features of *M. tuberculosis* dormancy.**

Keywords: dormancy, drug resistance, gene expression

Introduction

Isoniazid (isonicotinic acid hydrazide) has been the most widely used drug against *Mycobacterium tuberculosis* since recognition of its clinical activity in the early 1950s.[1] Isoniazid has potent bactericidal activity against *M. tuberculosis* grown *in vitro* and in animal models of tuberculosis, as well as in humans with active tuberculosis disease.[2] However, the drug has poor sterilizing activity relative to other antituberculosis agents such as rifampicin.[3–5] Thus, isoniazid has little or no activity against dormant *M. tuberculosis* grown under conditions of nutrient starvation[6] or progressive oxygen depletion *in vitro*.[7] In addition, isoniazid has reduced activity relative to rifampicin against *M. tuberculosis* in an *in vivo* granuloma model of dormancy.[8]

These observations may be explained by the drug's mechanism of action. Isoniazid is a pro-drug that is activated by the *M. tuberculosis katG*-encoded catalase-peroxidase enzyme.[9] In its active form, isoniazid inhibits multiple intracellular targets,[10–13] but its lethal effect is exerted by inhibition of mycolic acid synthesis.[14,15] Mycolic acids are high molecular weight, α-alkyl,

*Correspondence address. Center for Tuberculosis Research, Johns Hopkins University School of Medicine, 1550 Orleans Street, Room 106, Baltimore, MD 21231-1001, USA. Tel: +1-410-614-4225; Fax: +1-410-614-8173; E-mail: petros@jhmi.edu

β-hydroxy fatty acids, which are unique outer cell wall components of mycobacteria and other Actinomycetales.[16] Together with other lipids of the outer leaflet, mycolic acids constitute a very hydrophobic barrier,[17] and it is believed that disruption of this barrier results in loss of cellular integrity.[18] Isoniazid interrupts mycolic acid synthesis by binding tightly to the NADH-dependent enoyl acyl carrier protein reductase InhA,[19] a component of the fatty acid synthase II (FAS-II) system of mycobacteria, which is essential for fatty acid elongation. Recently, Vilcheze *et al*.[20] demonstrated that a single point mutation in *inhA* (S94A) was sufficient to confer 5-fold increased resistance to isoniazid, as well as inhibition of mycolic acid biosynthesis. Isoniazid appears to have potent activity against actively replicating *M. tuberculosis* but not against dormant organisms, perhaps because the latter are characterized by a non-replicating persistent state, which does not involve active cell wall synthesis. Alternatively, dormant organisms may be exposed to a hostile microenvironment in which the pro-drug cannot be converted to the bioactive form of the drug because of the lack of activity of *M. tuberculosis* KatG under these conditions.

Genome-wide expression analysis using microarrays provides a powerful means to study the adaptive survival strategies of bacteria in response to a variety of stress conditions.[21] *M. tuberculosis* gene expression in response to isoniazid exposure has been monitored *in vitro*,[22–25] revealing induction of several genes which encode proteins physiologically relevant to the drug's mode of action, as well as genes which are likely to mediate processes associated with the toxic consequences of the drug.[25] Likewise, the transcriptome of *M. tuberculosis* has been characterized in various *in vitro* models of dormancy, including under conditions of nutrient starvation[6] and progressive oxygen depletion,[26] as well as in an *in vivo* granuloma model of *M. tuberculosis* dormancy.[8]

Induction of a small group of genes directly relevant to the mechanism of action of isoniazid has been shown to be absent in an isoniazid-resistant, *katG*-deficient *M. tuberculosis* strain following low-dose isoniazid exposure ($\leq$1 mg/L),[25] and expression of these genes is detectable but diminished in another *katG*-deficient mutant after high-dose isoniazid exposure (10 mg/L).[27] We hypothesized that relative expression of isoniazid-regulated genes (IRGs) upon exposure to isoniazid could be used to predict bactericidal activity of the drug in various models of *M. tuberculosis* infection. Thus, we studied the global gene expression pattern of organisms treated with isoniazid in dormancy models of nutrient depletion[6] and progressive hypoxia *in vitro*,[7] as well in an *in vivo* hollow fibre model of dormancy,[8] and correlated gene expression patterns with bactericidal activity of isoniazid in these models. We also studied mycobacterial expression of the putative isoniazid transcriptional signature relative to isoniazid-induced killing of *M. tuberculosis* during the early and chronic phases of infection in the mouse aerosol and hollow fibre models.

Materials and methods

Strains

Wild-type *M. tuberculosis* H37Rv and a Δ*katG* mutant[28] [clinical isolate INH34 Δ(*furA-katG*) transformed with pAP1, containing intact *furA* and deletional interruption of *katG*, provided kindly by Stewart Cole, EPFL, Lausanne, Switzerland] were twice-passaged in mice. Cultures (25–50 mL) were grown to log-phase [optical density at 600 nm (OD_{600}) ~0.4] within 125 mL Ehrlenmeyer flasks containing Middlebrook 7H9 broth (Difco Laboratories) supplemented with 10% OADC (Becton–Dickinson), 0.05% Tween and 0.1% glycerol on a shaker at 37°C (shaking rate 180 rpm/min).

Progressive hypoxia model

M. tuberculosis H37Rv was grown to log-phase in Dubos Tween-albumin broth supplemented with 500 mg/L Methylene Blue and diluted to ~10^4 cfu/mL as determined by OD_{600}. A sufficient volume of culture yielding a ratio of head space air to medium volume (HSR) of 0.5 was transferred to individual test tubes containing a magnetic stir bar and sealed with a rubber stopper. The tubes were then incubated upright without shaking at 37°C and the magnetic stir bars spun at a speed sufficient to keep the organisms suspended uniformly throughout, but not enough to agitate the surface of the medium.[7] The reduction and decolorization of the Methylene Blue dye served as a visual indicator that the dissolved oxygen had dropped to below ~0.06% saturation, indicating entry of bacilli into non-replicating persistence (NRP) stage 2, in which organisms show phenotypic tolerance to isoniazid.[7] The day after dye colour change was used as a start time for isoniazid treatment for each biological replicate. Samples were collected at the designated time points by puncturing the rubber stopper with a 25-gauge needle while applying negative pressure. The lack of introduction of ambient oxygen into the hypoxia model tubes was ascertained by the maintenance of the decolorized dye state following sample collection.

Nutrient depletion model

After growth to log-phase (OD_{600} ~0.5), the *M. tuberculosis* cultures were diluted 100-fold in supplemented 7H9 Middlebrook broth, pelleted, washed twice with PBS and resuspended in PBS, as previously described,[6] with the exception that 0.05% Tween 80 was added to prevent clumping. Cultures were then incubated in 125 mL Ehrlenmeyer flasks (HSR > 0.5) at 37°C without shaking for 96 h to allow for reduction in mycobacterial respiration.[29] This was used as the isoniazid treatment start time for all replicates.

Antibiotic treatment in vitro

Isoniazid (100 μL, final concentration 1 mg/L) or vehicle was added to experimental and control samples, respectively, for each replicate in the nutrient depletion model, the progressive hypoxia model and exponentially growing cultures. Antibiotic was added to the progressive hypoxia samples by means of a 25-gauge needle and did not change the colour state of the Methylene Blue, indicating that the reduced oxygen tension had not been compromised. Samples were taken from each model at 0 and 6 h, as well as at days 1, 2, 3, 7 and 14 after isoniazid exposure, and plated onto 7H10 agar plates (Fisher Scientific) for cfu determination. Separate samples were taken 6 h after isoniazid exposure for RNA extraction.

Mouse infection

Six-week-old female, outbred SKH1 mice, which are hairless and immunocompetent, were used for all *in vivo* experiments.

To model dormant infection, mice were infected using the hollow fibre technique.[8] Briefly, exponential-phase *M. tuberculosis* was diluted to 10^5 cfu/mL as determined by OD_{600}, encapsulated into individual polyvinylidene difluoride fibres and implanted subcutaneously into mice. Three fibres were implanted into each mouse for global gene expression analysis studies, whereas two fibres were implanted into each mouse for bacterial enumeration and quantitative RT–PCR studies.

To model active infection, followed by chronic infection, mice were infected via the aerosol technique using a Glas-Col inhalation exposure system (Glas-Col, Terre Haute, IN, USA) according to the manufacturer's default settings. The nebulized sample consisted of log-phase *M. tuberculosis* diluted to $\sim 10^5$ cfu/mL as determined by OD_{600}, resulting in an approximate inoculum of 100 cfu/mouse lung.

Mice were maintained and procedures performed according to the protocol approved by the Institutional Animal Care and Use Committee at the Johns Hopkins University.

Antibiotic treatment in vivo

All mice received either isoniazid (25 mg/kg) or sham treatment comprising distilled water by oesophageal cannula. Mice were treated once daily for 5 of 7 days per week.

For global gene expression analysis studies, 15 hollow fibre-infected mice were each given either isoniazid or the sham treatment starting 14 days after implantation. Six hours after the third dose, hollow fibre contents (total volume per group = 300–600 μL) were recovered, pooled and snap-frozen in liquid nitrogen for RNA processing as described below.

For analysis of isoniazid bactericidal activity at different stages of *in vivo* infection, treatment was initiated at days 1, 14 or 42 after infection for mice infected either via aerosol or by the hollow fibre technique. For each of the three different treatment groups, three mice implanted with hollow fibres (six fibres total) and five mice infected by aerosol were sacrificed after the third daily antibiotic dose for mycobacterial RNA extraction. In each treatment group, three hollow fibre-infected mice and five aerosol-infected mice were also sacrificed at days 7 and 14 after treatment initiation. Fibre contents and homogenized mouse lungs were plated on 7H10 plates for cfu determination, and log-transformed cfu values were used to calculate averages and standard errors or standard deviations, respectively, for graphing purposes.

RNA extraction and processing

In vitro samples and hollow fibre contents were centrifuged at 3000 rpm for 10 min and the bacterial pellets were resuspended in TriZOL reagent (GIBCO/BRL). Lung samples were homogenized in TriZOL in glass homogenizers. *M. tuberculosis* membranes were disrupted using 0.1 mm zirconia/silica beads in a bead beater. *M. tuberculosis* RNA was recovered by centrifugation, chloroform extraction and isopropyl alcohol precipitation, and purified using RNeasy column (Qiagen) as previously described.[6,26] These steps were followed to extract mycobacterial RNA from both isoniazid-treated and -untreated samples in each particular experimental condition. A volume of 25 mL was used to extract RNA from *in vitro* samples and a volume of ~600 μL was used to extract RNA from hollow fibre samples. The entire organ (~1 mL) was used for RNA extraction from mouse lung samples.

Microarray analysis

Fluorescently labelled cDNA was generated using Powerscript (Clontech), using fluorescent dyes Cy3 and Cy5 for untreated control and isoniazid-treated samples, respectively, in each experimental condition. These cDNAs were competitively hybridized on microarray slides containing *M. tuberculosis* 70-mer oligo-nucleotides representing all open-reading frames annotated in the H37Rv genome sequencing project,[30] and fluorescence intensity data were collected with a GenePix 4000B scanner (Axon Instruments) with GenePix Pro 4.0 software. GenePix result files were loaded into the R statistical language using the limma package of bioconductor (www.bioconductor.org) for normalization and statistical analysis. Median spot intensities were calculated using the read.maimages function with weighted spots set to zero and normalized using the normalizeWithinArrays function with the non-linear printtiploess normalizing algorithm and the normexp background correction algorithm with a correction factor of 50. A linear model using the lmFit function was then applied to the normalized data and a Bayesian method for determining differential expression was applied using the eBayes function. Normalized microarray expression data deemed significant ($P < 0.01$) from *M. tuberculosis* exposed to isoniazid under the four different experimental conditions were clustered using Hierarchical Clustering Explorer 3.[31] Default settings were used to link individuals and measure similarity between clusters.

Quantitative RT–PCR

Prior to reverse transcription, RNA (100 ng) was treated with RNase-free DNase (Invitrogen) and subjected to 34 cycles of PCR to ensure that all DNA had been removed, as assessed by ethidium bromide-stained agarose gel analysis. After reverse transcription using gene-specific primers, cDNA corresponding to each transcript was subjected to 36 cycles of RT–PCR on the I-Cycler for quantification. The cycle threshold value (C_t) obtained for each gene of interest (GOI) was normalized with that of *sigA*, a housekeeping gene (HKG) with constant expression under different experimental conditions,[32] in order to obtain a normalized C_t [$NC_t = (HKG\ C_t) - (GOI\ C_t)$]. Levels of *sigA* were constant by microarray analysis in both isoniazid-

Table 1. Primers used in this study

ORF	Gene name	Sense primer	Antisense primer
Rv0129c	*fbpC*	aatatctgcaggtgccatcc	atgtcccagccgttgtagtc
Rv0341	*iniB*	gctagccagatcggtgtctc	atagcagcgccgttcaag
Rv1592c		ggctcaatggcactcttctt	tgcgtctaccgttgtcatct
Rv1772		tgggttcaacaggaggtagc	tatttcgaagaccggcaatc
Rv1854c	*ndh*	cttatttcggcaacgaccat	cgacaacggtgaatgtcagt
Rv2244	*acpM*	gtatcgagccgtccgagat	cttgacgccgtacttgtcct
Rv2245	*kasA*	ctaggtggagccgagaggat	caagctgcagaccgatcac
Rv2428	*ahpc*	cgttcagcaagctcaatgac	atcgggaagggtaacgtttt
Rv2703	*sigA*	ctcgacgctgaaccagacct	aggtcttcgtggtcttcgtc
Rv2763c	*dfrA*	gctgaggttgtcggttcact	cgacctcggtaacctcacat
Rv2846c	*efpA*	taggtttcatcccgttcgtc	tgaccaggttggggaagtag
Rv3139	*fadE24*	agccagcgacaacgactatt	ttcacatacgggacgacgta

ORF, open-reading frame.

treated and -untreated samples at each time point and in each model system. Fold regulation of individual genes following isoniazid exposure was calculated using the following formula: $2^{(NCt_S - NCt_C)}$, where S represents the isoniazid-treated sample and C represents the untreated control sample in each experimental condition. The gene-specific primers used for these experiments are listed in Table 1.

Results

Isoniazid activity against in vitro models

The bactericidal activity of isoniazid against *M. tuberculosis* was tested under three different conditions *in vitro*: (i) mid-exponential phase growth, (ii) progressive hypoxia[7] and (iii) nutrient depletion.[6] We hypothesized that isoniazid would have the most profound bactericidal effect against actively replicating organisms in mid-exponential phase and very limited activity against dormant organisms under conditions of progressive hypoxia and nutrient depletion.

As demonstrated in Figure 1a, isoniazid had significant bactericidal activity against exponentially growing organisms *in vitro*, resulting in a $\sim$3 $\log_{10}$ reduction in cfu by 48 h after initiation of drug exposure. The rise in cfu/mL in the isoniazid-treated group after 72 h of drug exposure may be explained by the selection of isoniazid-resistant mutants given the relatively high starting concentration of $>10^6$ organisms, which was chosen intentionally for subsequent microarray experiments, but which exceeds the spontaneous isoniazid resistance mutation rate of *M. tuberculosis in vitro*.[33]

When the dissolved oxygen content drops below 1%, slowly stirred *M. tuberculosis* grown in sealed containers with a 0.5 ratio of air to culture medium enters the microaerophilic NRP stage 1,[7] characterized by termination of DNA synthesis and thickening of the outer cell wall. As the dissolved oxygen drops to below $\sim$0.06% saturation, the bacilli enter NRP stage 2 and show reduced susceptibility to standard antituberculous drugs and increased susceptibility to the nitroimidazole drugs.[7,34] In our experiments, treatment with isoniazid or vehicle began 1 day after decolorization of the Methylene Blue dye, indicating entry of the organisms into NRP stage 2.[7] As expected for wild-type *M. tuberculosis* exposed to progressive hypoxia *in vitro*, the number of cfu/mL declined gradually over time, falling by 2 $\log_{10}$ over 14 days after entry into NRP stage 2 (Figure 1b). In contrast to the potent bactericidal activity of isoniazid against mid-exponential phase organisms, isoniazid had minimal activity against *M. tuberculosis* adapted to hypoxia, resulting in no mycobacterial killing, even after 14 days of treatment. Similarly, *M. tuberculosis* exposed to nutrient depletion conditions showed significantly reduced susceptibility to isoniazid, as cfu/mL in the drug-treated samples were within 1 $\log_{10}$ of those in the untreated samples after 14 days of treatment (Figure 1c).

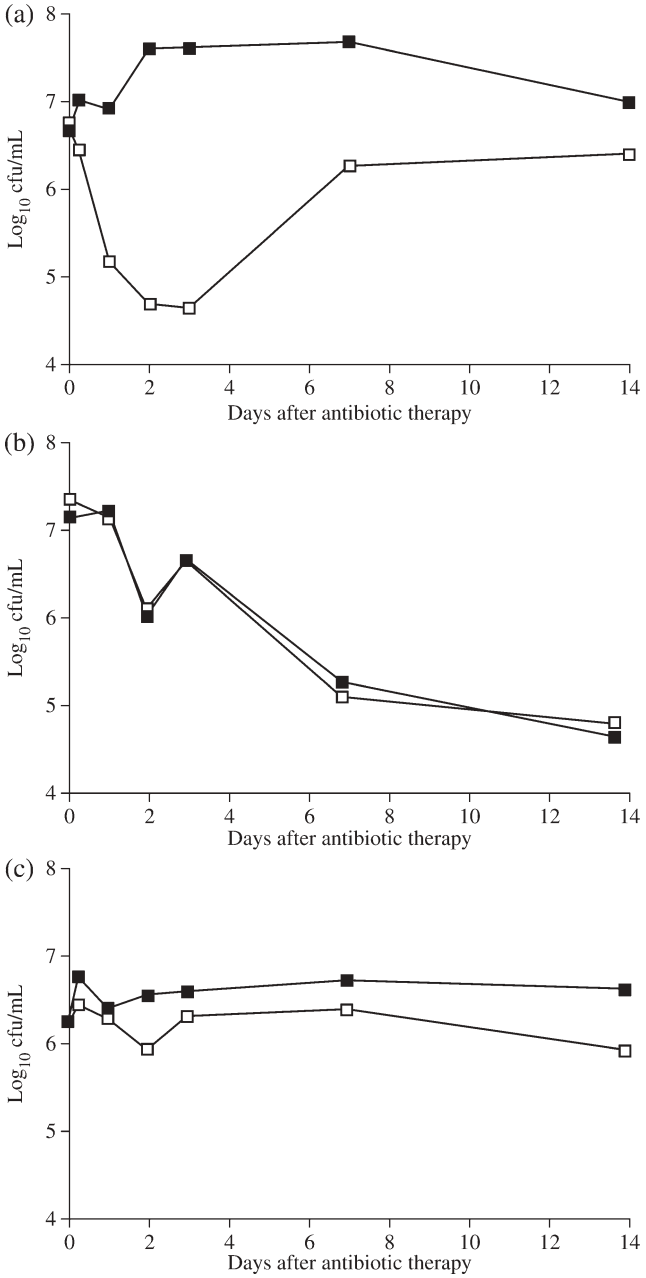

Figure 1. Bactericidal activity of isoniazid against *M. tuberculosis* under various conditions *in vitro*. Prior to isoniazid treatment, organisms were grown to mid-exponential phase (a), or were subjected to progressive hypoxia (b) or nutrient depletion (c). In each model, shaded squares represent untreated control samples, and open squares represent isoniazid-treated samples. Each experiment was repeated once, yielding similar results.

Isoniazid activity against M. tuberculosis in mouse lungs and in an in vivo granuloma model

The bactericidal activity of isoniazid was tested next at different stages of infection in the mouse aerosol model, as well as in a mouse granuloma model of extracellular persistence. In the latter model, organisms are encapsulated within semi-diffusible hollow fibres, which are implanted subcutaneously in mice. During the course of infection, there is progressive granulomatous inflammation surrounding the fibres, and within this microenvironment, the encapsulated organisms display a dormancy phenotype characterized by stationary-state cfu counts, decreased metabolic activity and increased susceptibility to rifampicin compared with isoniazid.[8] We hypothesized that isoniazid would have greater bactericidal activity during exponential growth of *M. tuberculosis* in mouse lungs than after the growth plateau

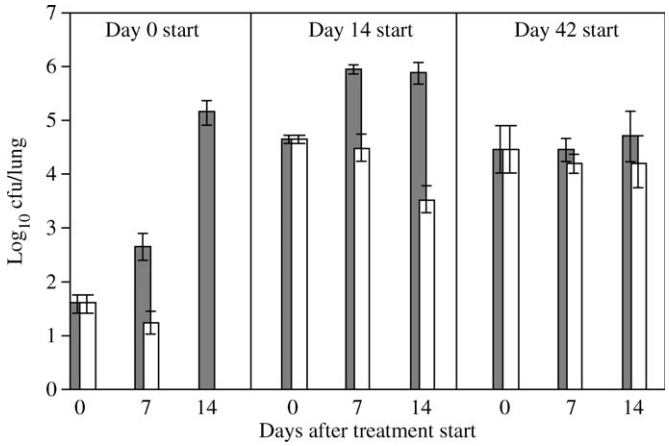

Figure 2. Bactericidal activity of isoniazid against *M. tuberculosis* in mouse lungs at different stages of infection. Shaded bars represent untreated control mice, and open bars represent isoniazid-treated mice.

resulting from the onset of adaptive immunity, and that isoniazid may have significant activity immediately after implantation of hollow fibres, but reduced activity following peri-fibre granuloma formation and entry of the organisms into a putatively dormant state.

Mice were infected with the same inoculum culture of *M. tuberculosis* H37Rv either via aerosol or by the hollow fibre technique,[8] resulting in ~50 cfu in mouse lungs and $\sim 10^4$ cfu in hollow fibres on day 1 after infection. Aerosol-infected and hollow fibre-infected mice were treated with isoniazid (25 mg/kg) daily by oesophageal cannula for a total of 14 days beginning on days 1, 14 and 42 of infection. Control animals in each group received daily sham gavage for a total of 14 days beginning at the same time points.

As shown in Figure 2, isoniazid showed potent activity against *M. tuberculosis* in mouse lungs when therapy was begun on day 1 after infection, resulting in non-cultivable lungs by 14 days after onset of therapy. The bactericidal activity of isoniazid was retained when therapy was initiated on day 14 after aerosol infection, as the number of cfu/lung was reduced by ~1.5 $\log_{10}$ after 14 days of therapy. In contrast, the bactericidal activity of isoniazid was greatly diminished when antibiotic therapy was initiated on day 42 after aerosol infection, such that there was no statistically significant difference in lung cfu between isoniazid-treated and -untreated mice 14 days after initiation of therapy.

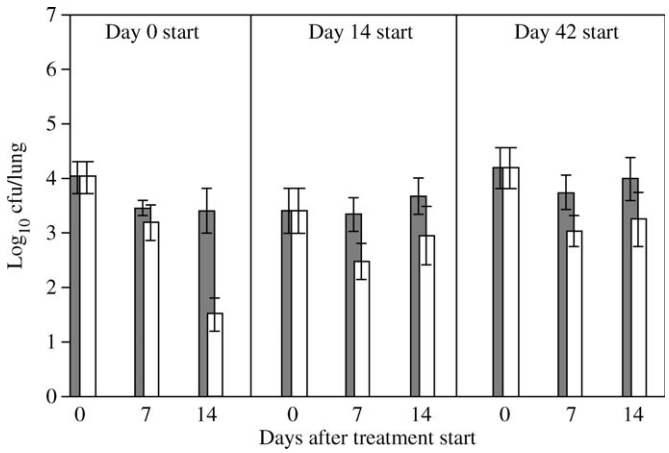

Figure 3. Bactericidal activity of isoniazid against subcutaneously implanted, hollow fibre-encapsulated *M. tuberculosis* at different stages of infection. Shaded bars represent untreated control mice, and open bars represent isoniazid-treated mice.

Isoniazid was highly active against hollow fibre-encapsulated organisms when therapy was initiated on day 1 after fibre implantation, resulting in an ~2 $\log_{10}$ reduction in cfu/fibre after 14 days of therapy (Figure 3). Isoniazid retained significant, albeit diminished, bactericidal activity against intra-fibre bacilli when therapy was initiated on day 14 after fibre implantation, and its activity was further reduced when therapy was initiated on day 42 after fibre implantation, resulting in a statistically insignificant difference in intra-fibre cfu between isoniazid-treated and -untreated groups 14 days after treatment initiation. These data are consistent with earlier findings that organisms in the *in vivo* granuloma model of extracellular persistence appear to gradually enter a dormant state characterized by up-regulation of the *dosR* regulation and reduced sensitivity to isoniazid.[8]

Global gene expression of M. tuberculosis in different phenotypic states following exposure to isoniazid

We hypothesized that the global gene expression pattern of dormant *M. tuberculosis* in response to isoniazid exposure would differ significantly from that of exponentially growing bacilli exposed to the drug *in vitro* and might provide insight into the phenotypic tolerance to isoniazid during dormancy.

The gene expression pattern of *M. tuberculosis* following isoniazid exposure was virtually unique in each model tested, with almost no overlap in genes significantly regulated ($P < 0.01$) between the models (Figure 4). As expected, the transcriptome of the Δ*katG* mutant in response to isoniazid during mid-exponential phase growth differed significantly from that of the wild-type strain under the same conditions. Specifically, 85 genes were found to be significantly differentially regulated ($P < 0.01$) in the exponentially growing Δ*katG* mutant after exposure to isoniazid relative to the untreated mutant. Of these, only one gene (Rv0283) was also significantly upregulated ($P < 0.01$) in isoniazid-treated, wild-type *M. tuberculosis* relative to untreated wild-type bacilli during log-phase growth. Of the 261 genes significantly regulated ($P < 0.01$) in exponentially growing organisms exposed to isoniazid, only 10 in the nutrient depletion model, 2 in the progressive hypoxia model and 1 in the hollow fibre model were coordinately regulated following isoniazid exposure. A full list of microarray data may be found in Table S1, available as Supplementary data at *JAC* Online (http://jac.oxfordjournals.org/).

M. tuberculosis expression of IRGs following exposure to the drug in the different models of infection

Consistent with prior work,[25] when mid-exponential phase organisms *in vitro* were exposed to isoniazid, we observed significant up-regulation of several genes encoding proteins physiologically relevant to the drug's mode of action, including the genes *fabD* (Rv2243), *acpM* (Rv2244), *kasA* (Rv2245), *kasB* (Rv2246) and *accD6* (Rv2247), which encode type II fatty acid synthase enzymes, as well as *fbpC*, which encodes trehalose dimycolyl transferase. In addition, we observed significant

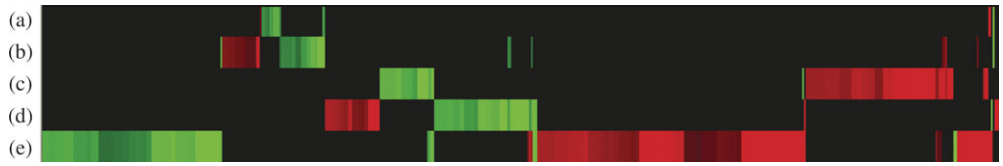

Figure 4. Graphical representation of *M. tuberculosis* H37Rv transcriptome following exposure to isoniazid ($P < 0.01$) under four different experimental conditions: (a) hollow fibre encapsulation *in vivo*; (b) progressive hypoxia *in vitro*; (c) nutrient depletion *in vitro*; and (e) exponential phase growth *in vitro*. (d) Global gene expression profile of log-phase Δ*katG* mutant exposed to isoniazid. Data were clustered using Hierarchical Clustering Explorer 3. Genes coloured red are up-regulated and those coloured green are down-regulated, whereas dark areas represent non-regulated genes.

Table 2. RT–PCR of *M. tuberculosis* IRGs in *in vitro* models

ORF	Gene	Log-phase	Nutrient depletion	Progressive hypoxia
Rv0129c	*fbpC*	4.09	2.38	0.64
Rv1854c	*ndh*	2.63	0.47	0.04
Rv2244	*acpM*	23.70	ND	ND
Rv2245	*kasA*	39.40	5.66	0.47
Rv2428	*ahpC*	21.11	1.15	0.26
Rv2763c	*dfrA*	0.23	0.42	0.05
Rv2846c	*efpA*	16.76	2.73	0.23
Rv3139	*fadE24*	25.99	6.73	0.29

ND, no data.
Values represent fold regulation.
Each data point represents *M. tuberculosis* gene expression 6 h after isoniazid exposure (1 mg/L) versus that of untreated cultures.

Table 3. RT–PCR of *M. tuberculosis* IRGs at different stages of infection *in vivo*

		Aerosol model		Hollow fibre model	
ORF	Gene	2 weeks	6 weeks	2 weeks	6 weeks
Rv0129c	*fbpC*	ND	0.62	19.70	1.23
Rv1854c	*ndh*	337.79	0.71	48.50	2.30
Rv2244	*acpM*	12.13	0.38	194.01	1.00
Rv2428	*ahpC*	477.71	ND	294.07	0.22
Rv2763c	*dfrA*	0.16	1.15	2.14	1.15
Rv2846c	*efpA*	ND	5.66	0.66	1.23
Rv3139	*fadE24*	1.52	0.33	222.86	1.07

ND, no data.
Values represent fold regulation.
RNA was extracted from mice 2 or 6 weeks after *M. tuberculosis* infection.
Each data point represents *M. tuberculosis* gene expression in animals 6 h after a single dose of isoniazid (25 mg/kg) versus that in untreated animals.

induction of other genes whose products are likely involved in processes associated with the toxic effects of isoniazid, including *efpA*, *fadE23* and *ahpC*. We used RT–PCR to confirm up-regulation of these genes (Table 2), which have been characterized previously as a transcriptional signature of isoniazid, since their expression is abrogated in a *katG*-deficient mutant.[25] Using RT–PCR, we also found increased expression of the NADH dehydrogenase gene *ndh* (Rv1854c), mutations in which have been identified in isoniazid-resistant clinical isolates.[35] However, log-phase *M. tuberculosis* exposed to isoniazid did not demonstrate up-regulation of *dfrA* (Rv2763c), which was recently implicated as a molecular target for isoniazid.[36]

Next, using RT–PCR, we explored *M. tuberculosis* expression of these IRGs following isoniazid exposure in the two *in vitro* models of dormancy. In contrast to isoniazid-treated log-phase organisms, hypoxia-adapted organisms exposed to isoniazid showed no differential regulation or even slight down-regulation of IRGs (Table 2). On the other hand, nutrient-depleted bacilli exposed to isoniazid showed mild up-regulation of IRGs, except for *ahpC*, which was not differentially regulated.

We next investigated the expression of IRGs by *M. tuberculosis* at different time points in the two *in vivo* models of infection. During the second week of unabated growth in mouse lungs, *M. tuberculosis* exposed to isoniazid revealed significant upregulation of IRGs, including *acpM* and *ahpC*. Similarly, when isoniazid was given 14 days after fibre implantation, hollow fibre-encapsulated bacilli showed significant up-regulation of IRGs, including *fbpC*, *acpM*, *ahpC* and *fadE24*. Interestingly, when isoniazid was initiated at 6 weeks after infection, upregulation of IRGs in the aerosol model was abrogated almost completely except for *efpA*, which was up-regulated 5.7-fold, and only *ndh* was up-regulated in the hollow fibre model of dormancy. Despite being significantly up-regulated in exponentially growing bacilli exposed to isoniazid, the gene *efpA*, which encodes an efflux pump, was not differentially regulated in hollow fibre-encapsulated bacilli at either time point after fibre implantation.

Expression of *M. tuberculosis ndh* was greatly increased in bacilli in mouse lungs when isoniazid was initiated 2 weeks after aerosol infection, but the gene was not differentially regulated when isoniazid therapy was started at 6 weeks of infection (Table 3). Similarly, *ndh* was highly up-regulated in hollow fibre-encapsulated organisms following initiation of isoniazid at 2 weeks of infection, but its expression declined significantly when isoniazid was started at 6 weeks after fibre implantation. *M. tuberculosis dfrA* was down-regulated more than 5-fold in bacilli in mouse lungs following isoniazid treatment at 2 weeks of infection and was not differentially regulated following isoniazid therapy at 6 weeks of infection. On the other hand, *dfrA* was slightly up-regulated in hollow fibre-encapsulated organisms following initiation of isoniazid at 2 weeks of infection and was not differentially regulated when isoniazid was started at 6 weeks after fibre implantation. RT–PCR was not successful for particular genes, perhaps because of low levels of specific mRNA present.

Discussion

We have confirmed that exposure of exponentially growing *M. tuberculosis* to the bactericidal drug isoniazid leads to a characteristic mycobacterial transcriptional profile reflecting the drug's mechanisms of action, as well as its related toxicities. Specifically, genes of the FAS-II operon, including *acpM* and *kasA*, are induced after isoniazid treatment as a consequence of the regulatory feedback mechanisms that sense the imbalance of full-length mycolates, which are depleted, and C24–C26 saturated fatty acids, which accumulate.[25] Other IRGs involved in mycolate transfer, fatty acid β-oxidation, detoxification and antibiotic efflux have been described previously.[25]

In order to gain insight into the lack of activity of isoniazid against dormant bacilli, we explored the transcriptional profile of *M. tuberculosis* in various phenotypic growth states after exposure to isoniazid. In general, lack of IRG expression by organisms following exposure to isoniazid correlated with lack of drug activity. Interestingly, isoniazid retained some activity against nutrient-depleted bacilli and induced mild up-regulation of some IRGs, including *kasA* of the FAS-II operon. These findings may be explained by the fact that isoniazid therapy was initiated 96 h after nutrient depletion, although it has been shown previously that oxygen consumption may continue to decrease in nutrient-starved bacilli as late as 17 days after depletion of nutrients.[29] The gradual metabolic downshift of nutrient-starved bacilli may reflect the initial availability of intracellular nutrient stores, which may become depleted upon prolonged nutrient starvation. Consistent with this hypothesis, Betts *et al*.[6] found that isoniazid 1 mg/L showed no activity against 6-week-starved cultures of *M. tuberculosis*.

There are several possibilities to help explain the correlation between phenotypic resistance to isoniazid and the lack of upregulation of IRGs in dormant bacilli following exposure to isoniazid. One plausible explanation is insufficient delivery of pro-drug to the intracellular compartment of *M. tuberculosis*. Penetration of the pro-drug into bacilli may be impeded by the formation of granulomatous lesions during late-stage infection *in vivo*. Contrary to this hypothesis, intra-fibre concentrations of isoniazid appear to closely parallel serum concentrations of the drug even after several weeks of infection in the mouse hollow fibre model (data not shown). In addition, isoniazid appears to penetrate host cells readily, as its antimycobacterial activity is essentially equivalent against intracellular *M. tuberculosis* and extracellular bacilli *in vitro*.[37] On the other hand, dormant *M. tuberculosis* may undergo structural or functional changes in its cell-wall preventing the intracellular entry or accumulation of pro-drug under certain stress conditions. Older studies using radioactively labelled isoniazid showed that bacilli in hypoxic conditions have reduced uptake of label, suggesting that isoniazid entry into *M. tuberculosis* involves oxygen-dependent active transport.[38] However, these findings may also be explained by reduced KatG activity under the same conditions, since intracellular accumulation of isoniazid appears to correlate with catalase-peroxidase activity.[39] Whereas KatG-dependent, isoniazid-derived radicals may be trapped inside bacilli, pro-drug may diffuse readily out of organisms when KatG is inactive, giving the impression of reduced isoniazid uptake.

Since KatG-mediated isoniazid activation appears to require oxygen,[40] and metal ions such as Cu^{2+} and Fe^{2+} enhance the activity of isoniazid,[33] enzymatic activity may be impaired under hypoxia and nutrient-depleted conditions, respectively. Hollow fibre-encapsulated bacilli show increased expression of the DosR regulon,[8] which is also up-regulated in *M. tuberculosis* exposed to hypoxic conditions *in vitro*,[41] suggesting that oxygen limitation may play a role in the microenvironment of the mouse hollow fibre model. On the other hand, the physicochemical microenvironment encountered by *M. tuberculosis* during chronic infection in mouse lungs remains poorly characterized, but does not appear to include tissue hypoxia.[42,43]

An alternative explanation for the dual phenomenon of phenotypic resistance to isoniazid and lack of induction of IRGs is that these organisms are in a non-replicating state in which cell turnover and *de novo* cell-wall synthesis are greatly diminished. Therefore, inhibition of the mycolic acid synthesis pathway may not lead to the imbalance of products and precursors necessary to trigger the characteristic isoniazid-associated transcriptional response or lead to mycobacterial cell death. Exposure of *M. tuberculosis* to progressive hypoxia[7] or prolonged nutrient-starvation conditions[29] appears to induce a phenotypic state characterized by severe growth limitation and metabolic quiescence. Similarly, extracellular *M. tuberculosis* within artificial granulomas in mice shows several features of dormant organisms, including stationary-state cfu counts, reduced metabolic activity, increased susceptibility to rifampicin rather than to isoniazid and up-regulation of the DosR regulon.[8] Although controversial, there is some evidence that during chronic infection in mouse lungs, persistent organisms may exhibit some features of dormancy. Specifically, Munoz-Elias *et al*.[44] showed that the viable bacillary counts and the bacterial chromosomal equivalents in the lungs of chronically infected mice do not diverge over time, suggesting that the stable number of bacterial cfu in the lungs during chronic infection represents a static equilibrium between host and pathogen.

Although inhibition of DNA synthesis by isoniazid had been observed long ago,[10] only recently was a mechanism of action for this phenomenon proposed. Argyrou *et al*.[36] cloned and overexpressed the *M. tuberculosis* gene encoding dihydrofolate reductase (DHFR), *dfrA*, in *M. smegmatis* and demonstrated a 2-fold increase in MIC. *M. tuberculosis* DHFR was shown to selectively bind and co-crystallize with an active isoniazid metabolite, which is distinct from that which binds InhA.[45] We did not find consistent induction of *dfrA* after isoniazid exposure of metabolically active, dividing organisms. Confirmation of DHFR as a molecular target of isoniazid requires further biochemical and genetic work, and mutations in *dfrA* have yet to be reported among isoniazid-resistant clinical isolates of *M. tuberculosis*.

As with other IRGs, we found markedly enhanced expression of *ndh* following isoniazid treatment of *M. tuberculosis* when organisms were in a metabolically active, replicating state, but not when organisms were in a putatively dormant state. Mutations in *ndh* were first shown in *M. smegmatis* to confer resistance to isoniazid and ethionamide.[46] Subsequently, *ndh* mutations were detected in almost 10% of isoniazid-resistant *M. tuberculosis* clinical isolates, which did not contain mutations in *katG*, *inhA* or *kasA*.[35] Defective NADH dehydrogenase, which normally oxidizes NADH and transfers electrons to quinones of the respiratory chain, could lead to an increased ratio of NADH/NAD, which may interfere with KatG-mediated peroxidation of the drug or displace the isoniazid/NAD adduct from the InhA active site.[46]

In conclusion, we have confirmed that a specific group of genes directly relevant to the inhibitory and toxic effects of isoniazid constitutes a transcriptional signature of the drug. Isoniazid-induced expression of this transcriptional signature is lost in genetically susceptible, phenotypically resistant organisms regardless of the particular conditions used to induce this dormant state, suggesting a common underlying physiology. Although we cannot exclude the possibility that there may be different types of mycobacterial dormancy based on our results, the reduced susceptibility of bacilli to the bactericidal drug isoniazid, as well as lack of expression of IRGs upon exposure to the drug, may be defining features of *M. tuberculosis* dormancy.

Acknowledgements

We gratefully acknowledge the support of NIAID 5K08AI064229, NO1 30036, R01 36973, R01 37856, R01 43846 and the Potts Memorial Foundation. Microarray slides were obtained through NIH, NIAID Contract No. HHSN266200400091C, entitled 'Tuberculosis Vaccine Testing and Research Materials', which was awarded to Colorado State University.

Funding

Funding was obtained from the following grants: NIAID 5K08AI064229, NO1 30036, R01 36973, R01 37856, R01 43846 and the Potts Memorial Foundation.

Transparency declarations

None to declare.

Supplementary data

Table S1 is available as Supplementary data at *JAC* Online (http://jac.oxfordjournals.org/).

References

1. Robitzek EH, Selikoff IJ. Hydrazine derivatives of isonicotinic acid (rimifon marsilid) in the treatment of active progressive caseous-pneumonic tuberculosis; a preliminary report. *Am Rev Tuberc* 1952; **65**: 402–28.

2. Jindani A, Aber VR, Edwards EA *et al.* The early bactericidal activity of drugs in patients with pulmonary tuberculosis. *Am Rev Respir Dis* 1980; **121**: 939–49.

3. Dickinson JM, Mitchison DA. Experimental models to explain the high sterilizing activity of rifampin in the chemotherapy of tuberculosis. *Am Rev Respir Dis* 1981; **123**: 367–71.

4. Grosset J, Lounis N, Truffot-Pernot C *et al.* Once-weekly rifapentine-containing regimens for treatment of tuberculosis in mice. *Am J Respir Crit Care Med* 1998; **157**: 1436–40.

5. Mitchison DA. Mechanisms of the action of drugs in the short-course chemotherapy. *Bull Int Union Tuberc* 1985; **60**: 36–40.

6. Betts JC, Lukey PT, Robb LC *et al.* Evaluation of a nutrient starvation model of *Mycobacterium tuberculosis* persistence by gene and protein expression profiling. *Mol Microbiol* 2002; **43**: 717–31.

7. Wayne LG, Hayes LG. An *in vitro* model for sequential study of shiftdown of *Mycobacterium tuberculosis* through two stages of nonreplicating persistence. *Infect Immun* 1996; **64**: 2062–9.

8. Karakousis PC, Yoshimatsu T, Lamichhane G *et al.* Dormancy phenotype displayed by extracellular *Mycobacterium tuberculosis* within artificial granulomas in mice. *J Exp Med* 2004; **200**: 647–57.

9. Zhang Y, Heym B, Allen B *et al.* The catalase-peroxidase gene and isoniazid resistance of *Mycobacterium tuberculosis*. *Nature* 1992; **358**: 591–3.

10. Gangadharam PR, Harold FM, Schaefer WB. Selective inhibition of nucleic acid synthesis in *Mycobacterium tuberculosis* by isoniazid. *Nature* 1963; **198**: 712–4.

11. Brennan PJ, Rooney SA, Winder FG. The lipids of *Mycobacterium tuberculosis* BCG: fractionation, composition, turnover and the effects of isoniazid. *Ir J Med Sci* 1970; **3**: 371–90.

12. Zatman LJ, Kaplan NO, Colowick SP *et al.* Effect of isonicotinic acid hydrazide on diphosphopyridine nucleotidases. *J Biol Chem* 1954; **209**: 453–66.

13. Bekierkunst A. Nicotinamide-adenine dinucleotide in tubercle bacilli exposed to isoniazid. *Science* 1966; **152**: 525–6.

14. Takayama K, Wang L, David HL. Effect of isoniazid on the *in vivo* mycolic acid synthesis, cell growth, and viability of *Mycobacterium tuberculosis*. *Antimicrob Agents Chemother* 1972; **2**: 29–35.

15. Winder FG, Collins PB. Inhibition by isoniazid of synthesis of mycolic acids in *Mycobacterium tuberculosis*. *J Gen Microbiol* 1970; **63**: 41–8.

16. Brennan PJ, Nikaido H. The envelope of mycobacteria. *Annu Rev Biochem* 1995; **64**: 29–63.

17. Draper P. The outer parts of the mycobacterial envelope as permeability barriers. *Front Biosci* 1998; **3**: D1253–61.

18. Barry CE 3rd, Lee RE, Mdluli K *et al.* Mycolic acids: structure, biosynthesis and physiological functions. *Prog Lipid Res* 1998; **37**: 143–79.

19. Banerjee A, Dubnau E, Quemard A *et al. inhA*, a gene encoding a target for isoniazid and ethionamide in *Mycobacterium tuberculosis*. *Science* 1994; **263**: 227–30.

20. Vilcheze C, Wang F, Arai M *et al.* Transfer of a point mutation in *Mycobacterium tuberculosis inhA* resolves the target of isoniazid. *Nat Med* 2006; **12**: 1027–9.

21. Jenner RG, Young RA. Insights into host responses against pathogens from transcriptional profiling. *Nat Rev Microbiol* 2005; **3**: 281–94.

22. Betts JC, McLaren A, Lennon MG *et al.* Signature gene expression profiles discriminate between isoniazid-, thiolactomycin-, and triclosan-treated *Mycobacterium tuberculosis*. *Antimicrob Agents Chemother* 2003; **47**: 2903–13.

23. Boshoff HI, Myers TG, Copp BR *et al.* The transcriptional responses of *Mycobacterium tuberculosis* to inhibitors of metabolism: novel insights into drug mechanisms of action. *J Biol Chem* 2004; **279**: 40174–84.

24. Waddell SJ, Stabler RA, Laing K *et al.* The use of microarray analysis to determine the gene expression profiles of *Mycobacterium tuberculosis* in response to anti-bacterial compounds. *Tuberculosis (Edinb)* 2004; **84**: 263–74.

25. Wilson M, DeRisi J, Kristensen HH *et al.* Exploring drug-induced alterations in gene expression in *Mycobacterium tuberculosis* by microarray hybridization. *Proc Natl Acad Sci USA* 1999; **96**: 12833–8.

26. Sherman DR, Voskuil M, Schnappinger D *et al.* Regulation of the *Mycobacterium tuberculosis* hypoxic response gene encoding α-crystallin. *Proc Natl Acad Sci USA* 2001; **98**: 7534–9.

27. Fu LM, Shinnick TM. Understanding the action of INH on a highly INH-resistant *Mycobacterium tuberculosis* strain using Genechips. *Tuberculosis (Edinb)* 2007; **87**: 63–70.

28. Pym AS, Domenech P, Honore N *et al*. Regulation of catalase-peroxidase (KatG) expression, isoniazid sensitivity and virulence by *furA* of *Mycobacterium tuberculosis*. *Mol Microbiol* 2001; **40**: 879–89.

29. Loebel RO, Shorr E, Richardson HB. The influence of adverse conditions upon the respiratory metabolism and growth of human tubercle bacilli. *J Bacteriol* 1933; **26**: 167–200.

30. Cole ST, Brosch R, Parkhill J *et al*. Deciphering the biology of *Mycobacterium tuberculosis* from the complete genome sequence. *Nature* 1998; **393**: 537–44.

31. Seo J, Shneiderman B. Interactively exploring hierarchical clustering results. *IEEE Comput* 2002; **35**: 80–6.

32. Manganelli R, Dubnau E, Tyagi S *et al*. Differential expression of 10 sigma factor genes in *Mycobacterium tuberculosis*. *Mol Microbiol* 1999; **31**: 715–24.

33. Winder F. The antibacterial action of streptomycin, isoniazid, and PAS. In: Barry V, ed. *Chemotherapy of Tuberculosis*. London: Butterworth, 1964; 111–49.

34. Wayne LG, Sramek HA. Metronidazole is bactericidal to dormant cells of *Mycobacterium tuberculosis*. *Antimicrob Agents Chemother* 1994; **38**: 2054–8.

35. Lee AS, Teo AS, Wong SY. Novel mutations in ndh in isoniazid-resistant *Mycobacterium tuberculosis* isolates. *Antimicrob Agents Chemother* 2001; **45**: 2157–9.

36. Argyrou A, Vetting MW, Aladegbami B *et al*. *Mycobacterium tuberculosis* dihydrofolate reductase is a target for isoniazid. *Nat Struct Mol Biol* 2006; **13**: 408–13.

37. Suter E. Multiplication of tubercle bacilli within phagocytes cultivated *in vitro*, and effect of streptomycin and isonicotinic acid hydrazide. *Am Rev Tuberc* 1952; **65**: 775–6.

38. Youatt J. The uptake of isoniazid by washed cell suspensions of *Mycobacteria* and other organisms. *Aust J Exp Biol Med Sci* 1958; **36**: 223–33.

39. Wimpenny JW. Effect of isoniazid on biosynthesis in *Mycobacterium tuberculosis* var. *bovis* BCG. *J Gen Microbiol* 1967; **47**: 379–88.

40. Zabinski RF, Blanchard JS. The requirement for manganese and oxygen in the isoniazid-dependent inactivation of *Mycobacterium tuberculosis* enoyl reductase. *J Am Chem Soc* 1997; **119**: 2331–2.

41. Park HD, Guinn KM, Harrell MI *et al*. Rv3133c/dosR is a transcription factor that mediates the hypoxic response of *Mycobacterium tuberculosis*. *Mol Microbiol* 2003; **48**: 833–43.

42. Tsai MC, Chakravarty S, Zhu G *et al*. Characterization of the tuberculous granuloma in murine and human lungs: cellular composition and relative tissue oxygen tension. *Cell Microbiol* 2006; **8**: 218–32.

43. Aly S, Wagner K, Keller C *et al*. Oxygen status of lung granulomas in *Mycobacterium tuberculosis*-infected mice. *J Pathol* 2006; **210**: 298–305.

44. Munoz-Elias EJ, Timm J, Botha T *et al*. Replication dynamics of *Mycobacterium tuberculosis* in chronically infected mice. *Infect Immun* 2005; **73**: 546–51.

45. Rozwarski DA, Grant GA, Barton DH *et al*. Modification of the NADH of the isoniazid target (InhA) from *Mycobacterium tuberculosis*. *Science* 1998; **279**: 98–102.

46. Miesel L, Weisbrod TR, Marcinkeviciene JA *et al*. NADH dehydrogenase defects confer isoniazid resistance and conditional lethality in *Mycobacterium smegmatis*. *J Bacteriol* 1998; **180**: 2459–67.